

# Noninvasive Visualization of Three-Dimensional Atrial Electrical Excitation Using Anterior and Posterior Magnetocardiogram

K Ogata<sup>1</sup>, A Kandori<sup>1</sup>, T Miyashita<sup>1</sup>, K Tsukada<sup>2</sup>, S Nakatani<sup>3</sup>, W Shimizu<sup>3</sup>,  
H Kanzaki<sup>3</sup>, K Miyatake<sup>3</sup>, S Yamada<sup>4</sup>, S Watanabe<sup>4</sup>, I Yamaguchi<sup>4</sup>

<sup>1</sup> Hitachi Ltd., Central Research Laboratory, Tokyo, Japan

<sup>2</sup> Department of Electrical and Electronic Engineering, University of Okayama, Okayama, Japan

<sup>3</sup> National Cardiovascular Center, Osaka, Japan

<sup>4</sup> Institute of Clinical Medicine, University of Tsukuba, Ibaraki, Japan

## Abstract

*The aim of our work is to visualize three-dimensional (3-D) images of atrial excitation. We obtained these images by projecting the anterior and posterior current-arrow map (CAM), derived from a magnetocardiogram (MCG), onto a 3-D standard heart model. We generated the projected CAM (PCAM) of early and late atrial depolarization phases for fourteen healthy subjects. During early and late atrial excitation, the high-current areas of all subjects were in the right atrium of the anterior surface, and the left atrium of the posterior surface. The averaged ratio of the maximal current value of the early p-wave to the maximal current value of the late p-wave for all subjects was  $0.9 \pm 0.2$ . Furthermore, the averaged maximal current directions of the early and late p-wave were  $78 \pm 15$  and  $165 \pm 17$  degrees, respectively. Thus, we found that the PCAM could provide separated images of the left and right atrial excitations.*

## 1. Introduction

Magnetocardiograms (*MCGs*) are a novel technology that can produce images of the cardiac electrical current. An *MCG* measures the weak cardiac magnetic field generated by the adults [1] or by fetuses [2], non-invasively. A two-dimensional (*2-D*) current-arrow map (*CAM*) [3] was developed as a practical method of calculating pseudo cardiac currents from an *MCG*. The *CAM* provides the foundation of a new diagnosis system for various heart diseases [4, 5]. Furthermore, we were able to visualize multiple excited areas during ventricular excitation using anterior and posterior *CAMs* [6]. Recently, a novel method for projecting anterior and posterior *CAMs* onto a three-dimensional (*3-D*) standard heart model [7] was developed. This method is called *PCAM* and gives us a clear view of the cardiac electrical

current.

The aim of our work is to visualize *3-D* images of atrial electrical excitation using *PCAM*. We used a superconducting quantum interference device (*SQUID*) system to measure the axial components of the anterior and posterior *MCGs*. The anterior and posterior *CAMs* were calculated by taking spatial derivatives of the measured anterior and posterior *MCGs*. The *3-D* standard heart model was generated from the magnetic resonance (*MR*) images of three healthy subjects.

This standard heart model was then adjusted to the optimal position for each subject using information on the heart's position. This information took the form of the sinus node coordinates, which were calculated from *MCG* signals. After adjusting the base current values of the anterior and posterior *CAMs*, they were projected onto the positionally corrected standard heart model. We applied *PCAM* to obtain a cardiac-current image of the atrial depolarization phase (p-wave) of fourteen healthy subjects.

## 2. Measurement

### 2.1. MCG measurements

Figure 1 shows the conventional configuration for measuring *MCG* signals. We used a *Low-Tc SQUID* system (MC-6400, Hitachi High-Technologies Corporation), with 64 co-axial gradiometers to measure the *MCG* signals, which were axial components to the chest wall (see figure 2). The magnetic flux resolution of all gradiometers was better than  $20 \text{ fT/Hz}^{1/2}$ . The *SQUID* sensors were laid out in an  $8 \times 8$  matrix, with a pitch of 25 mm, and the measurement area was  $175 \times 175$  mm. For the anterior chest wall measurement, a sensor (7, 3) was placed above the position of the xiphoid process. For the posterior chest wall measurement, a sensor (7, 6) was placed directly underneath the position of the xiphoid process. The *MCG* signals were acquired at a sampling

frequency of 1 kHz and passed through band-pass (0.1-100 Hz) and power-line noise filters. The measurement period was 30 s, and the *MCG* signals for all pulses over this period were averaged. To adjust the phases of the anterior and posterior *MCGs*, we simultaneously measured the Lead II electrocardiogram (*ECG*) signals.

## 2.2. Heart MRI measurements

To visualize the 3-D structure of the entire surface of the heart, *MR* images were recorded by scanning 300 x 300 mm coronal planes, vertically separated by 6 mm using an *MRI* system (Magnex 100 (1T), Shimadzu Corporation). We used *ECG* triggering (R-wave peak) to control *MR* image capture. Body motions associated with the heartbeat were theoretically corrected by using *ECG* triggering. The *MR* examination for each subject was completed within about 30 minutes.

## 3. Method

We generated cardiac excitation images by projecting anterior and posterior *CAMs*, which are derived from anterior and posterior *MCG*, onto a 3-D standard heart model [7].

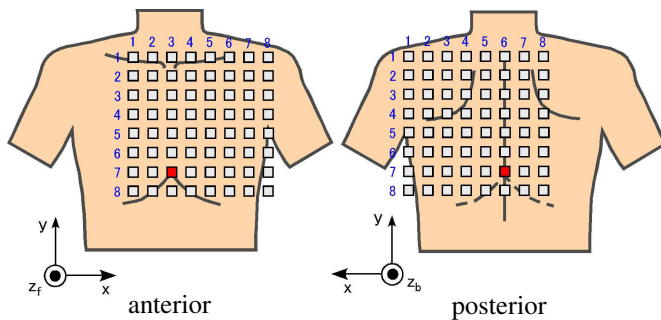


Figure 1. Configuration for MCG measurement.



Figure 2. MCG system (MC-6400, Hitachi High-Technologies Corporation).

We made the standard heart model from chest *MR* images of the chest of three healthy subjects. After the *MR* images were obtained, heart-outline points were extracted from each image and 3-D heart models for each subject were made from these points. The centroid of the heart model was calculated from all heart-outline points. Then, the distances from the centroid to each point were obtained. The averages were calculated from these distances for the three subjects and were used to generate the 3-D standard heart model.

The standard heart model was adjusted to the optimal position for each subject using information about the heart's position, in the form of the sinus node coordinates. The coordinates are obtained by applying an equivalent current dipole (*ECD*) algorithm [8] to the *MCG* signals at the beginning of the p-wave. Therefore, the optimal position of the standard heart model was determined by superposing the position of the sinus node on the standard heart model from the calculated position of the corresponding current dipole.

The *CAM* represents a 2-D pseudo cardiac electrical current [3]. The current arrows of *CAM* ( $I = (I_x, I_y)$ ) were calculated by taking orthogonal partial derivatives of the axial components to the chest wall of the cardiac magnetic field. In other words, the *CAM* was obtained from  $I_x = dB_{z,n} / dy$  and  $I_y = -dB_{z,n} / dx$ , here,  $B_{z,n}$  represents the axial components of the measured cardiac magnetic field. Furthermore, the magnitude of the current arrow  $|I|$  was derived from  $|I| = (I_x^2 + I_y^2)^{1/2}$ .

The anterior and posterior *CAMs* were projected onto the anterior and posterior surfaces of the positionally adjusted standard heart model, respectively. However, the projected *CAM* (*PCAM*) showed a discontinuous current pattern at the junction of the anterior and posterior surfaces of the standard heart model, because the base currents of the anterior and posterior *CAMs* were quite different. This is because the distance between the heart and anterior measurement plane is not equal to the distance between the heart and posterior measurement plane. Therefore, we used a weighting coefficient  $W$ , which adjusted the base currents of the anterior and posterior *CAMs*. The weighting function was obtained by equalizing the anterior and posterior *CAM* on the outermost heart outline for the *xy* plane.

To evaluate the *PCAM* of the atrial depolarization phase (p-wave), we extracted the maximal current value and direction. The maximal current value reflects the amplitude of electrical current in the myocardium. The maximal current direction reflects the electrical axis of the heart. Therefore, *PCAM* could be verified by investigating these values in healthy subjects. The maximal current directions were quantified based on the definition of the current arrow direction (see Figure 3).

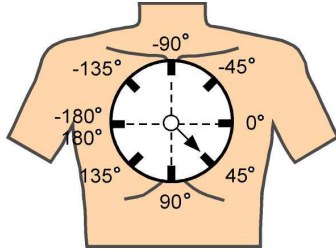


Figure 3. Definition of current arrow directions.

## 4. Results

### 4.1. PCAM for typical healthy subjects

Figure 4 shows the *MCG* waveforms of the anterior and posterior measurements for one healthy subject. Figures 4 (a) and (b) show the posterior and anterior overlapped waveforms of all 64 channels. We can see that the *MCG* waveforms were composed of the p-wave, QRS-complex, and T-wave. The lines in Figs. 4 (a) and (b) represent the two phases (#1: early p-wave, #2: late p-wave) when the two *PCAM* images in figures 5 (a) and (b) were taken. Figures 5 (a) and (b) show *PCAMs* during the p-wave. The arrows indicate the current direction, and the color-map indicates the magnitude of the current vector.

The high-current area of the *PCAM* during the early p-wave stage (right atrial excitation, 80 ms) was in the right atrium of the anterior surface of the standard heart model, and the current flow was in the inferior direction in the upper right. During the late p-wave (left atrial excitation, 110 ms), the high-value area (red area) was in the left atrium of the posterior surface. For all subjects, the high-current areas of the early and late p-wave were in the right atrium of the anterior surface and the left atrium of the posterior surface, respectively.

### 4.2. Maximal current value and direction of *PCAM*

Table 1 shows the maximal current values and directions during early and late p-wave. Moreover, the ratio of maximal current value of early and late p-wave appear in Table 1, which also shows the average maximal current values, directions, the averaged ratio of the maximal current value of the early p-wave to the maximal current value for the fourteen subjects (male: twelve, female: two, average age $\pm$ SD: 37 $\pm$ 5). During the early p-wave stage, the maximal current values for all subjects was in a range from 17 to 84 pT/m, and the average current value was 38 $\pm$ 15 pT/m. The maximal current direction during early p-wave was in a range of 17 to 95 degrees. The average current direction was 78  $\pm$  15 degrees. During the late p-wave stage, the maximal current values for all subjects was in a range from 29 to

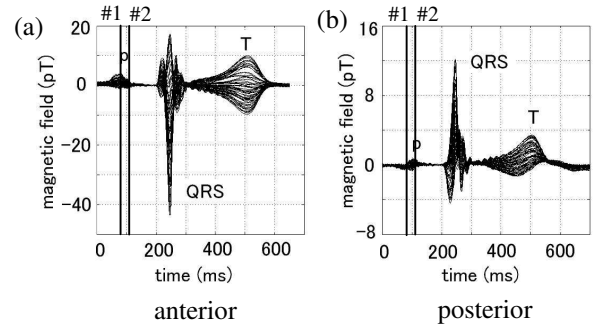


Figure 4. *MCG* waveforms for a healthy subject ((a) front plane, (b) back plane).

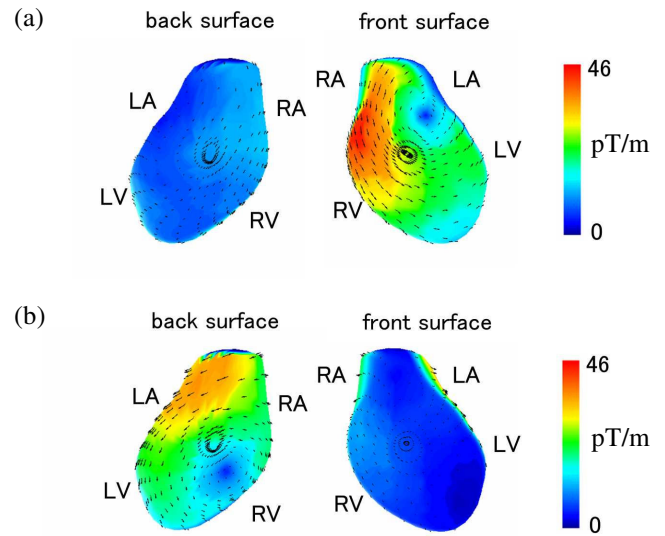


Figure 5. *PCAMs* for a healthy subject. (a) early p-wave (right atrial excitation), (b) late p-wave (left atrial excitation). RA: Right Atrium, LA: Left Atrium, RV: Right Ventricle, LV: Left Ventricle.

Table 1 Maximal current values and directions of early and late p-wave for fourteen healthy subjects.

No.	Maximal current value (nT/m)		ratio	Maximal current direction (degree)	
	early p-wave	late p-wave		early p-wave	late p-wave
N1	50	45	1.1	82	144
N2	39	68	0.6	96	151
N3	71	60	1.2	89	180
N4	17	26	0.7	82	161
N5	38	37	1.0	92	162
N6	21	30	0.7	65	129
N7	22	40	0.6	79	171
N8	29	47	0.6	57	146
N9	23	31	0.7	24	185
N10	48	40	1.2	92	159
N11	84	61	1.4	90	84
N12	26	29	0.9	66	233
N13	29	43	0.7	17	165
N14	32	30	1.1	96	156
average	37.8	41.9	0.9	77.7	164.8
SD	14.7	10.4	0.2	15.2	16.9

68 pT/m, and the current direction during early p-wave was in the range of the average current value of  $42 \pm 10$  pT/m. The maximal current direction during the late p-wave stage was in the range of 84 to 233 degrees. The average current direction was  $165 \pm 17$  degrees. Furthermore, the averaged ratio of the maximal current value of right atrium to the maximal current value of the left atrium was  $0.9 \pm 0.2$ .

## 5. Discussion

To visualize the cardiac electrical current in an atrial myocardium, we projected *CAMs*, calculated from *MCG* signals that corresponded to the p-wave, onto a 3-D standard heart model. The electrical activity in the p-wave should reflect right- and left atrial excitation [9]. The *PCAMs* during the p-wave are seen in Figs. 5 (a) and (b). During the early p-wave stage, the high-current area was in the right atrium of the model's anterior surface. In the later stage, the region of greatest activity shifted towards the left atrium of the model's posterior surface. Similar results during the p-wave for healthy subjects were reported using the anterior and posterior 2-D *CAMs* [10].

To evaluate the validity of the *PCAM*, we extracted the maximal current values and directions of early and late p-wave for fourteen healthy subjects (Table 1). The averaged ratio of the maximal current value of early p-wave to the maximal current value of late p-wave was  $0.9 \pm 0.2$ . This indicates that the current value of right atrial excitation was almost equal to the current value of left atrial excitation. On the other hand, the averaged directions of maximal current of the early and late p-wave were quite different. Therefore, the anterior and posterior surfaces of the *PCAM* reflected the different excitation activity in the heart. These results show that the *PCAM* can produce a clear view of the actual electrical excitation in the left and right atrium during p-wave excitation.

## 6. Conclusions

We developed a *PCAM* method for use with a 3-D standard heart model. This method was applied to visualize early and late atrial excitation in fourteen healthy subjects. During early and late atrial excitation, high-current areas of all subjects were in the right atrium of the anterior surface and left atrium of the posterior surface, respectively. The averaged ratio of the maximal current value of the early p-wave to the maximal current value of the late p-wave for all subjects was  $0.9 \pm 0.2$ . Furthermore, the averaged maximal current directions of the early and late p-wave were  $78 \pm 15$  and  $165 \pm 17$

degrees, respectively. We found that the *PCAMs* for healthy subjects reflected electrical excitation in the left and right atrium.

## References

- [1] Tsukada K, Haruta Y, Adachi A, Ogata H, Komuro T, Ito T, Takada Y, Kandori A, Noda Y, Terada Y, and Mitsui T: Multichannel SQUID system detecting tangential components of the cardiac magnetic field. *Rev Sci Instrum* 66: 5085, 1995
- [2] Horigome H, Siono J, Shigemitsu S, Asaka M, Matsui A, Kandori A, Miyashita T, and Tsukada K: Detection of cardiac hypertrophy in the fetus by approximation of the current dipole using magnetocardiography. *Pediatr Res* 50: 242, 2001
- [3] Miyashita T, Kandori A, and Tsukada K: Construction of tangential vectors from normal cardiac magnetic field components: Proc 20th Int Conf IEEE/EMBS (Hong Kong): 520, 1998
- [4] Kandori A, Shimizu W, Yokokawa M, Kamakura S, Miyatake K, Murakami M, Miyashita T, Ogata K, and Tsukada K: Reconstruction of action potential of repolarization in patients with congenital long-QT syndrome. *Phys Med Biol* 49: 2103, 2004
- [5] Kanzaki H, Nakatani S, Kandori A, Tsukada K, and Miyatake K: A new screening method to diagnose coronary artery disease using multichannel magnetocardiogram and simple exercise. *Basic Res Cardiol* 98: 124, 2003
- [6] Tsukada K, Mitsui T, Terada Y, Horigome H, and Yamaguchi I: Noninvasive visualization of multiple simultaneously activated regions on torso magnetocardiographic maps during ventricular depolarization. *J Electrocardiol* 32: 305, 1999
- [7] Ogata K, Kandori A, Miyashita T, Tsukada K, Yamada S, Shimizu W, Nakatani S, Miyatake K, and Yamaguchi I: Projecting cardiac current images onto a 3-D standard heart model. Proc 20th Int Conf IEEE/EMBS (Cancun): 517, 2003
- [8] Nomura M, Nakaya Y, Saito K, Kishi F, Watatsuki T, Myoshi H, Nishikado B, Bando S, Ito S, Nishitani H, Wada M, Fujita S, and Tamura I: Noninvasive localization of accessory pathways by magnetocardiographic imaging. *Clin Cardiol* 17: 239, 1994
- [9] Durrer D, van Dam R, Freud GE, Janse MJ, Meijler FL, and Arzbaeher RC: Total Excitation of the isolated human heart. *Circulation* 41: 899, 1970
- [10] Sato M, Terada Y, Mitsui T, Miyashita T, Kandori A and Tsukada K: Visualization of atrial excitation by magnetocardiogram. *Int J Card Imag* 18: 305, 2002

Address for correspondence

Kuniomi Ogata

1-280, Higashi-koigakubo, Kokubunji city, Tokyo, 185-8601, Japan

k-ogata@rd.hitachi.co.jp